



HAL
open science

Low frequency acoustic pressure measurements based on a Fabry-Perot refractometer

Amazigh Rezki, Zaccaria Silvestri, Jean-Pierre Wallerand, Cécile Guianvarc'h,
Marc Himbert

► **To cite this version:**

Amazigh Rezki, Zaccaria Silvestri, Jean-Pierre Wallerand, Cécile Guianvarc'h, Marc Himbert. Low frequency acoustic pressure measurements based on a Fabry-Perot refractometer. TC16 Conference 2022, Oct 2022, Cavtat-Dubrovnik, Croatia. pp.1-5, 10.21014/tc16-2022.008 . hal-03986945

HAL Id: hal-03986945

<https://cnam.hal.science/hal-03986945>

Submitted on 13 Feb 2023

HAL is a multi-disciplinary open access archive for the deposit and dissemination of scientific research documents, whether they are published or not. The documents may come from teaching and research institutions in France or abroad, or from public or private research centers.

L'archive ouverte pluridisciplinaire **HAL**, est destinée au dépôt et à la diffusion de documents scientifiques de niveau recherche, publiés ou non, émanant des établissements d'enseignement et de recherche français ou étrangers, des laboratoires publics ou privés.

LOW FREQUENCY ACOUSTIC PRESSURE MEASUREMENTS BASED ON A FABRY PEROT REFRACTOMETER

A. Rezki¹, Z. Silvestri¹, J-P. Wallerand¹, C. Guianvarc’h², M. Himbert¹

¹ LNE-CNAM, 1 rue Gaston Boissier, Paris, France, amazigh.rezki@lecnam.net
LOMC UMR CNRS 6294, 75 rue Bellot, Le Havre, France, ²cecile.guianvarch@univ-lehavre.fr

Abstract:

This paper presents the development, the operating principle, and the experimental results of an innovative technique for the measurement of acoustic pressures in the range of 40 mHz up to 5 Hz. This new measurement technique is based on the use of a Fabry Perot refractometer in which the air density variations related to an acoustic wave can be tracked and determined by measuring the optical frequency variations of a laser locked on a longitudinal mode of the Fabry Perot cavity. This approach covers a wider range in the low and infrasonic frequencies compared to conventional sensors.

Keywords: Fabry Perot; infrasonic pressure; refractometry; optical microphone; opto-acoustic sensor

1. INTRODUCTION

Until now, the monitoring of powerful events related to natural causes (e.g., tsunamis, volcanoes) is achieved by infrasonic waves measurements. However, the sensors used to perform these measurements, are designed for specific and local applications with limited operating ranges. Moreover, for a metrological purpose, we shall notice the BIPM database still misses Calibration and Measurement Capabilities (CMC) at infrasonic pressure frequencies below 2 Hz, i.e., from static pressure to acoustic pressure [1]. There is thus a particular need to develop a primary calibration method to extend the frequency range from quasi-static pressure (40 mHz) to acoustic pressure (20 Hz) that is not yet covered by National Metrology Institutes (NMI).

The primary standards for sound pressure measurement are laboratory standards microphones, which must be calibrated using the pressure reciprocity calibration method as specified in the International Electrotechnical Commission (IEC) Standard 61094-2:2009 [2].

However, for infrasound applications, the extension of the reciprocity method to the lowest frequencies of interest is not straightforward and

results in implementation problems particularly because of low signal-to-noise ratios, acoustic leakages, and unsatisfactory models used in their implementation [3], [4].

On the other hand, with the latest revision of the International System of Units in 2019 [5], an alternative way is offered to realize the pascal unit without any mechanical actuator but rather depends on the thermodynamic aspect of a gas. By calculating the refractivity of a gas inside a refractometer using frequency measurements of a laser beam, its density can be derived from the Lorentz–Lorenz equation [6]. In the case where air is used, semi empirical equations such as the revised formulae of Elden’s and Ciddor’s [7]-[9] can then be used to deduce the pressure inside the refractometer. Knowing other atmospheric parameters such as relative humidity (RH), temperature (T), and carbon dioxide (CO₂) concentration is then required anyway.

For the measurement of air density, we use a Fabry Perot (FP) based refractometer which is essentially a technique for evaluating gas refractivity, molar density, and pressure. Such a refractometer has already been implemented in some NMIs to realize absolute manometers [10], [11]. Nevertheless, for performing absolute static pressure measurements, this technique implies several corrections which are mainly due to the variation of the cavity length coming from material ageing, pressure, and temperature instabilities. These long-term drifts require an extensive treatment in the case of static pressure measurement, using a gas modulation method [12] for instance, but not necessarily for relative pressure variations.

In this paper, the FP refractometer is used as an opto-acoustic sensor to measure dynamic pressure in the range of 40 mHz up to 5 Hz. A similar technique has been developed for example by Kaniak *et al.* [13], but these works focus on the ultrasonic frequency range without locking the laser frequency on the top of a resonant peak of the FP.

2. BASIC PRINCIPLES OF THE METHOD

A. FABRY PEROT REFRACTOMETER

The heart of the refractometer comprises a single Fabry Perot cavity which is a plano-concave optical resonator of 100 mm long and 22 mm internal diameter, with a Zerodur® spacer chosen for its low coefficient of thermal expansion which is given by the manufacturer as $1.6 \times 10^{-8}/^{\circ}\text{C}$. The cylindrical resonator shown on Figure 1, which contains twelve ventilation holes to allow air flow, is placed in a aluminum cylinder enclosed inside a stainless-steel 10 L vacuum chamber [14].

To avoid long term drifts of the cavity, the FP refractometer is regulated with a stability of ± 1 mK over 1 hour. The air temperature inside the refractometer is measured by a calibrated Pt100.

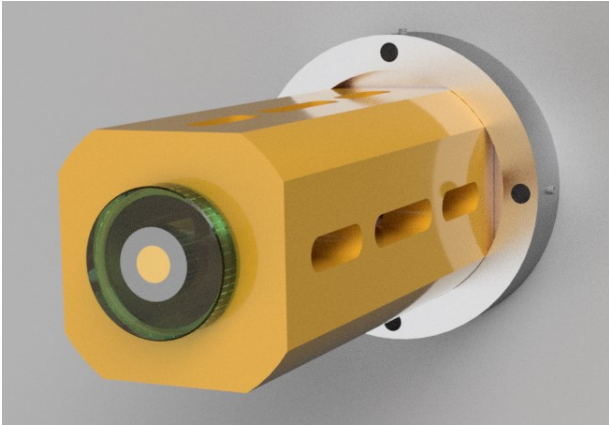


Figure 1: Fabry Perot cavity composed of Zerodur® spacer and fused silica mirrors at each end

B. PRESSURE AND OPTICAL REFRACTIVITY

The frequency of the laser beam is locked on the top of a resonant peak of the FP, which is a TEM_{00} cavity mode. The frequency of the laser beam ν_L is then given by:

$$\nu_L = k \times \frac{c}{2nL} = \frac{c}{n\lambda}, \quad (1)$$

where k is a mode number, c the speed of light in vacuum, λ the wavelength of the laser beam, and n the refractive index of air between both mirrors of the FP. The laser wavelength remains thus constant in the cavity provided that the distance L between the two mirrors is constant.

The air density variations related to the generated acoustic pressure lead to proportional variations in the air refractive index. This periodic change of air index implies a periodic variation of the frequency of the laser to keep its wavelength constant between both mirrors of the cavity. According to equation (1), a variation of air

refractive index Δn induces a variation of laser frequency $\Delta \nu$ such that:

$$\Delta \nu = -\nu_L \times \frac{\Delta n}{n}. \quad (2)$$

In practice, $\Delta \nu$ is determined by measuring the beat frequency at GHz scale with respect to a reference laser that is frequency locked on a hyperfine component of molecular iodine transition [15].

As the refractometer is filled with ambient air, we use Edlen's equation and updates, which directly link air refractive index to temperature, pressure, partial pressure of water, and CO_2 content to a lesser extent. The updated Edlen equation done by Bönsch and Potulski [8] relates in a simple way these quantities:

$$\Delta n = k(\lambda) \cdot D(\Delta T, \Delta p) \quad (3)$$

$k(\lambda)$ being a wavelength-dependent parameter.

A variation of Δn in air refractivity induced by a variation of pressure Δp , temperature ΔT and a lesser extent to water pressure variation. In case of dynamic pressure generation at a given frequency, a variation of air index at this frequency is induced. If in addition a temperature variation at this frequency occurs, this should be taken into account and corrected to deduce the pressure variation from air index variation. This case will be discussed in part 4 of the paper.

3. WORKING PRINCIPLE

The infrasonic pressure is generated here by a repeatable and controllable electrodynamic loudspeaker, transmitting pure harmonic signals. The vertical displacement of the loudspeaker's diaphragm causes a volume variation, and then pressure variation, in the enclosure. The sinusoidal acoustic pressure propagates to the measuring transducers through flexible pipes. The dimensions of the pipes and enclosures constituting the measurement system are much smaller than the lowest acoustic wavelength in the frequency range of interest here (i.e., about 68 m at 5 Hz).

In order to check the validity of our optical sensor by comparing its results with those obtained with other reference sensors, the same acoustic waves are measured by a calibrated piezo-resistive barometer (Druck Pace1000) and a calibrated condenser measurement microphone (Brüel & Kjaer type 4193 and its power supply type 2829) as shown in the following Figure 2.

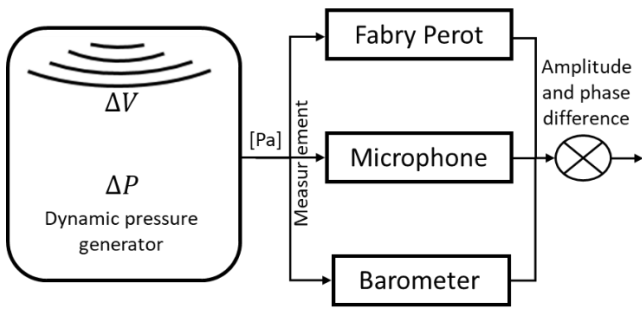


Figure 2: Basic principles of the comparison calibration system carried out

A more detailed view of the global experience, implemented at the LNE-Cnam is presented in the Figure 3, from the infrasonic pressure generation to its measurement by the different pressure sensors.

The FP refractometer, subjected to the acoustic pressure field, is crossed by a 532 nm beam of a frequency doubled Nd:YAG laser, that makes several round trips depending on the reflection coefficients of the mirrors. If the distance between the cavity mirrors L is a multiple of half the wavelength, i.e. $L = k\lambda/2$ (as shown in Eq. (1)),

the waves inside the cavity add up in a constructive interference. The light at the output of the FP is converted into an electrical signal, that has a form of an Airy function, using a photodiode.

This electrical signal is demodulated by a lock-in amplifier and thus transformed into an error signal which is the first derivative of the Airy signal. The zero value of the center of the derivative is selected as the lock point by activating the PID controller. The PID signal, which is considered as the correcting signal, is added to the modulation signal, and sent to the piezoelectric part (PZT) of the laser to provide a correction at any time.

As the frequency of the laser is locked on the transmission peak of the FP, each change in air density is then tracked. This frequency is measured in practice using a beat frequency with a reference laser which is another 532 nm frequency doubled Nd:YAG laser locked on a hyperfine component of a molecular iodine transition, as represented in Figure 3, [15], [16].

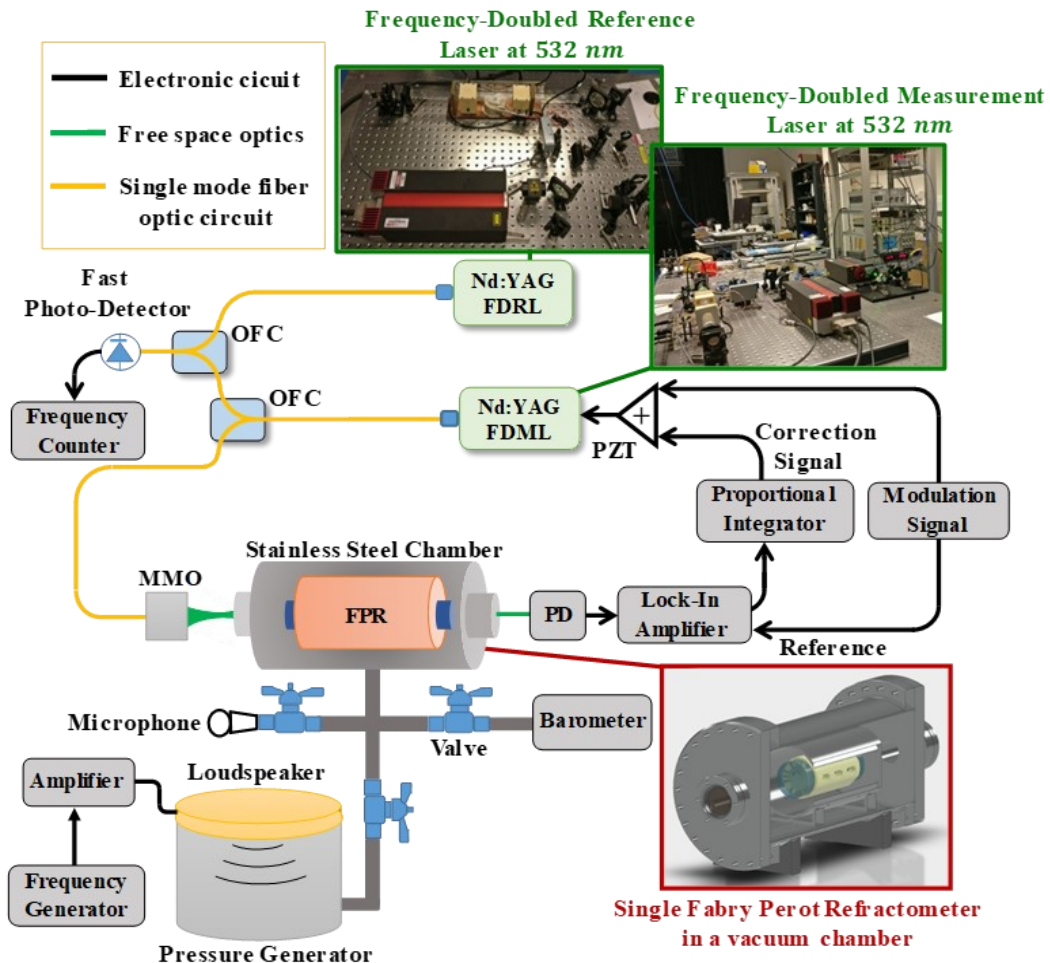


Figure 3: Optical measurement system of infrasonic waves. Components include: Optical Fiber Coupler (OFC), Piezoelectric Transducer (PZT), photodetector (PD), Mode Matching Optics (MMO)

4. EXPERIMENTAL RESULTS AND DISCUSSIONS

To experimentally check the validity of the whole measurement set up, from the acoustic pressure generation to its measurement by the three pressure sensors, dynamic waves are generated over an operating range of the system (40 mHz – 1.1 Hz) as shown in the Figure 4 (but in practice we can reach 5 Hz).

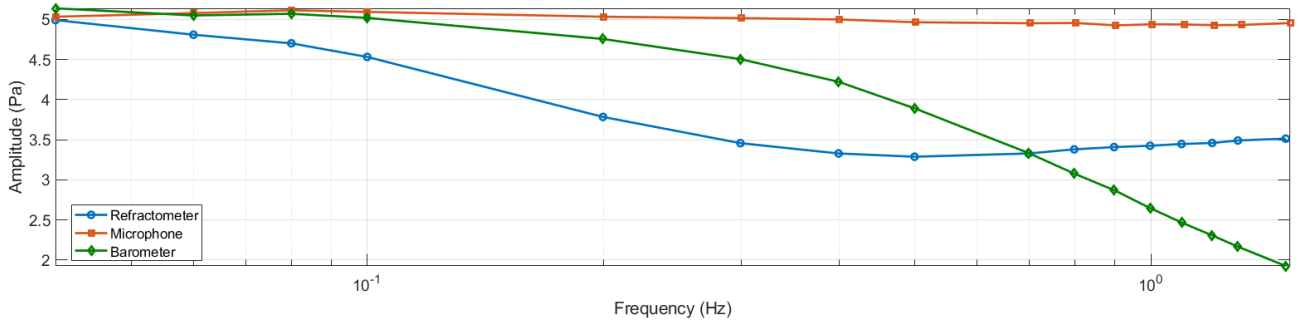


Figure 4: Amplitude of infrasonic pressure obtained with a calibrated microphone, a calibrated barometer and a FP refractometer

The calibrated microphone used is considered to give the true pressure variation amplitude. Figure 4 shows that the pressure remains constant over the entire operating range, independent of frequency.

The refractometer allows us to deduce air pressure variations in the FP cavity from air refractivity measurements. However, air refractivity variation depends also on temperature variation along the laser beam.

Indeed, in a “free field”, a dynamic pressure wave generates an acoustic temperature wave denoted P and τ respectively. In adiabatic regime, these two quantities are linked by the following relation:

$$\tau = \frac{T_0 \gamma - 1}{P_0 \gamma} p, \quad (4)$$

T_0 being the ambient temperature, P_0 the ambient pressure and γ the ratio of isobaric and isochoric heat capacities [3].

This relationship enables to calculate temperature variation due to pressure variation. Then this temperature should be compensated from the air index equation, to compensate the apparent amplitude decrease of the infrasonic pressure measured with the refractometer above 1 Hz.

On the other hand, the rigid walls of the cavity impose isothermal boundary conditions and, as a consequence, acoustic temperature gradients along the axis and radius of the cavity. The amplitude of these gradients is strongly related to the depth of the thermal boundary layers δ_h , given by:

The pressure amplitude measured by the three sensors is the same to within a few millipascals at very low frequencies. The intrinsic characteristic of the microphone causes its measurement to be out of phase with those of other pressure sensors.

The barometer’s results allow us to check the validity of this system in the lowest frequency range. As expected, above about 100 mHz, the barometer is not able to follow the acoustic pressure variations. In the higher frequency range of interest, we shall check the validity of all-optical sensor’s results against those of the microphone.

$$\delta_h = \sqrt{\frac{\alpha_T}{\pi f}}, \quad (5)$$

α_T being the the thermal diffusivity of the enclosed gas [3], with a value of $\alpha_T \approx 2.11 \times 10^{-5} m^2 \cdot s^{-1}$ for a cylinder.

The Figure 5 shows the evolution of the depth of the thermal boundary layers in terms of frequency:

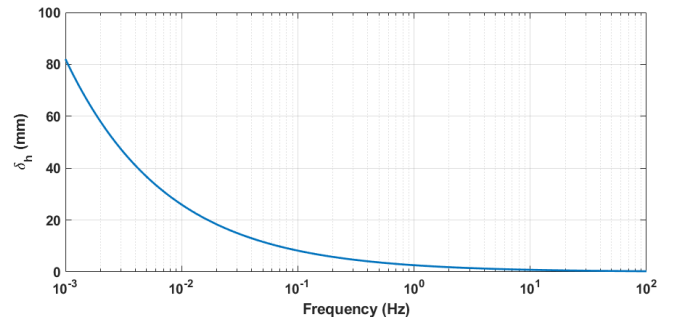


Figure 5: Evolution of thermal boundary layers as a function of frequency

In the lowest frequency range (i.e., below 10 mHz), the thermal boundary layers are large than the internal cavity diameter (22 mm). In this case, the isothermal boundary conditions are dominant, and no temperature corrections should be necessary to the refractometer’s pressure measurements, which is consistent with results plotted on Fig. 4.

Between these two “extreme” and ideal regimes (isothermal and adiabatic), the relationship between temperature variations and acoustic pressure is more complex but can be modelled [3]. The

implementation and validation of the associated corrections in our all-optical infrasonic measurement system is in progress.

5. SUMMARY

This paper describes a feasibility experiment for a primary calibration of low-frequency acoustic pressure sensors over a range from 40 mHz to 5 Hz using a Fabry Perot cavity. This opto-acoustic sensor, based on the all-optical effect, shows a deviation in the pressure measurements from the reference microphone measurements, which is compensated by taking into account the temperature variations coupled to acoustic pressure. The first tests with these corrections make us optimistic about the ability of this technique for the calibration of acoustic sensors in a low frequency range.

This work is part of the project Infra-AUV. The project 19ENV03 Infra-AUV has received funding from the EMPIR programme cofinanced by the participating states and from the European Union's Horizon 2020 research and innovation programme.

The authors would like to thank R. Karcher and P. Vincent from CEA-DAM for their collaboration and for providing the acoustic pressure generator.

6. REFERENCES

- [1] "Résolution 1 (2018) - BIPM." <https://www.bipm.org/fr/committees/cg/cgpm/26-2018/resolution-1> (accessed Jun. 02, 2022).
- [2] "IEC 61094-2:2009 | IEC Webstore." Online [Accessed 20220206]: <https://webstore.iec.ch/publication/4486>
- [3] P. Vincent, D. Rodrigues, F. Larssonier, C. Guianvarc'h, and S. Durand, "Acoustic transfer admittance of cylindrical cavities in infrasonic frequency range," *Metrologia*, vol. 56, no. 1, p. 015003, Feb. 2019. DOI: [10.1088/1681-7575/aace28](https://doi.org/10.1088/1681-7575/aace28)
- [4] R. Barham and M. Goldsmith, "The application of the NPL laser pistonphone to the international comparison of measurement microphones," *Metrologia*, vol. 44, p. 210, May 2007. DOI: [10.1088/0026-1394/44/3/007](https://doi.org/10.1088/0026-1394/44/3/007)
- [5] M. Stock, R. Davis, E. de Mirandés, and M. J. T. Milton, "The revision of the SI—the result of three decades of progress in metrology," *Metrologia*, vol. 56, no. 2, p. 022001, Apr. 2019. DOI: [10.1088/1681-7575/ab0013](https://doi.org/10.1088/1681-7575/ab0013)
- [6] J. A. Stone and A. Stejskal, "Using helium as a standard of refractive index: correcting errors in a gas refractometer," *Metrologia*, vol. 41, no. 3, pp. 189–197, Apr. 2004. DOI: [10.1088/0026-1394/41/3/012](https://doi.org/10.1088/0026-1394/41/3/012)
- [7] P. E. Ciddor, "Refractive index of air: new equations for the visible and near infrared," *Appl. Opt.*, vol. 35, no. 9, p. 1566, Mar. 1996. DOI: [10.1364/AO.35.001566](https://doi.org/10.1364/AO.35.001566)
- [8] G. Bönsch and E. Potulski, "Measurement of the refractive index of air and comparison with modified Edlén's formulae," *Metrologia*, vol. 35, no. 2, pp. 133–139, Apr. 1998. DOI: [10.1088/0026-1394/35/2/8](https://doi.org/10.1088/0026-1394/35/2/8)
- [9] K. P. Birch and M. J. Downs, "An Updated Edlén Equation for the Refractive Index of Air," *Metrologia*, vol. 30, no. 3, pp. 155–162, Jan. 1993. DOI: [10.1088/0026-1394/30/3/004](https://doi.org/10.1088/0026-1394/30/3/004)
- [10] P. F. Egan, J. A. Stone, J. K. Scherschligt, and A. H. Harvey, "Measured relationship between thermodynamic pressure and refractivity for six candidate gases in laser barometry," *Journal of Vacuum Science & Technology A*, vol. 37, no. 3, p. 031603, May 2019. DOI: [10.1116/1.5092185](https://doi.org/10.1116/1.5092185)
- [11] K. Jousten et al., "Perspectives for a new realization of the pascal by optical methods," *Metrologia*, vol. 54, no. 6, pp. S146–S161, Dec. 2017. DOI: [10.1088/1681-7575/aa8a4d](https://doi.org/10.1088/1681-7575/aa8a4d)
- [12] I. Silander, T. Hausmaninger, M. Zelan, and O. Axner, "Gas modulation refractometry for high-precision assessment of pressure under non-temperature-stabilized conditions," *Journal of Vacuum Science & Technology A*, vol. 36, no. 3, p. 03E105, May 2018. DOI: [10.1116/1.5022244](https://doi.org/10.1116/1.5022244)
- [13] G. Kaniak et al., "Enhanced non-contact ultrasonic testing using an air-coupled optical microphone," in 2020 IEEE SENSORS, Rotterdam, Netherlands, Oct. 2020, pp. 1–4. DOI: [10.1109/SENSORS47125.2020.9278623](https://doi.org/10.1109/SENSORS47125.2020.9278623)
- [14] Z. Silvestri, D. Bentouati, P. Otał, and J.-P. Wallerand, "Towards an improved helium-based refractometer for pressure measurements," *ACTA IMEKO*, vol. 9, no. 5, Dec. 2020, pp. 305 – 309. DOI: [10.21014/acta_imeko.v9i5.989](https://doi.org/10.21014/acta_imeko.v9i5.989)
- [15] P. Jungner, M. D. Eickhoff, S. D. Swartz, J. Ye, J. L. Hall, and S. B. Waltman, "Stability and absolute frequency of molecular iodine transitions near 532 nm," San Jose, CA, United States, Apr. 1995, p. 22. DOI: [10.1117/12.208229](https://doi.org/10.1117/12.208229)
- [16] S. Picard et al., "Comparison of 127I2-stabilized frequency-doubled Nd:YAG lasers at the Bureau International des Poids et Mesures," *Appl Opt*, vol. 42, no. 6, Feb. 2003, pp. 1019–1028. DOI: [10.1364/ao.42.001019](https://doi.org/10.1364/ao.42.001019)